18th International Conference on Structural Mechanics in Reactor Technology (SMiRT 18)
Beijing, China, August 7-12, 2005
SMiRT18-G11-7

HIGH-TEMPERATURE CRACK GROWTH BEHAVIOR OF HIGH-CHROMIUM STEELS

Yukio TAKAHASHI*
Central Research Institute of Electric Power Industry
Iwado-Kita 2-11-1, Komae-shi, Tokyo, Japan
Phone: +81-3-3480-2111
Fax: +81-3-3430-2410
E-mail: yukio@criepi.denken.or.jp

Toshihide IGARI
Mitsubishi Heavy Industries, Ltd.
Fukahori-machi, Nagasaki-shi, Tokyo, Japan
Phone: +81-95-834-2143
Fax: +81-95-834-2175
E-mail: toshihide_igari@mhi.co.jp

Fumiko KAWASHIMA
Mitsubishi Heavy Industries, Ltd.

Shingo DATE
Mitsubishi Heavy Industries, Ltd.

Norihiro ISOBE
Hitachi, Ltd.

Takuya ITOH
Ishikawajima-Harima Heavy Industries Co., Ltd.

Yasutaka NOGUCHI
Sumitomo Metal Industries, Ltd.

Kenichi KOBAYASHI
Chiba University

Masaaki TABUCHI
National Institute for Materials Science

ABSTRACT

High-chromium steels are widely used in recent fossil power plants because of their excellent high-temperature strength. They are also regarded as promising candidates for structural materials for high-temperature nuclear power plants such as liquid metal-cooled fast reactors and high-temperature gas-cooled reactors. Their crack growth property is often required to evaluate the structural integrity under the presence of detected or postulated flaws. In addition to fatigue crack growth property, crack growth property under creep and creep-fatigue loading is important because of high operating temperatures of these plants. As a study in the working group organized in Japan Society of Materials Science, experimental and analytical studies have been conducted on high-temperature crack growth property of representative high-chromium steels. Researchers from plant manufacturers, utilities and universities participated to this activity. Temperature- and specimen -dependency of crack growth properties in terms of J-integral type fracture mechanics parameters were examined in detail. Standard equations were derived to estimate crack growth rate as a functions of these parameters. Effect of constraint on creep crack growth behavior was found to be quite large.

Keywords: high-chromium steel, high-temperature, crack growth, fatigue, creep, creep-fatigue

1. INTRODUCTION

Because of their excellent high-temperature strength, high-chromium steels are widely used in recent fossil power plants to increase thermal efficiency by rising operating temperature and pressure. Good thermal property made them candidates for structural materials for high-temperature nuclear power plants such as liquid metal-cooled fast reactor and high-temperature gas-cooled reactors under design. In addition to basic properties regarding tensile, creep and fatigue strength required in structural design, their crack growth property is indispensable to evaluate the structural integrity of the components. In addition to fatigue crack growth property, crack growth property under creep and creep-fatigue loading is important because of high operating temperatures of these plants.

As a study in the working group organized in Japan Society of Materials Science, experimental and analytical studies have been conducted on crack growth property of high-chromium steels. Researchers from plant manufacturers, utilities and universities participated to the working group and performed crack growth tests based on their routine test technologies. Fatigue, creep and creep-fatigue crack growth tests were conducted for modified 9Cr-1Mo steel and HCM12A and relations between fracture mechanics parameters and crack growth rate were discussed.

2. TESTED MATERIALS

As a high-chromium steel most widely used in fossil power plants in Japan and other countries, modified 9Cr-1Mo steel (P91) was selected as the main test material. However, HCM12A (P122) which was also started to use in recent plants was also tested to study the material-dependence of crack growth behavior. Both materials were produced as hot-rolled plates of 50mm thickness and subjected to normalization and tempering. Post weld heat treatment was also applied before mechanical tests. Chemical compositions and mechanical property of these materials are shown in Tables 1 and 2, respectively. Both materials have similar microstructure designated as tempered martensite and mechanical behavior is generally similar.

Tensile tests, fatigue tests and creep tests were conducted for smoothed round-bar specimens to grasp uniaxial deformation behavior under various conditions. HCM12A showed higher tensile and creep strength than modified 9Cr-1Mo steel but difference tended to decrease with increase in temperature and decrease in stress. Cyclic deformation behavior and creep deformation behavior were modeled by Ramberg-Osgood equation and Blackburn-type creep strain equation

3. FATIGUE CRACK GROWTH TESTS

3.1 Test Method

14 fatigue crack growth tests were conducted at high temperatures in four organizations. Both center-cracked tension (CCT) and compact tension (CT) specimens were used. Specimen geometries are shown in Figure 1. Test conditions are summarized in Table 3. Tests were conducted at 550℃ or 650℃ for modified 9Cr-1Mo steel and at 600℃ for HCM12A. Many tests were conducted at load control but in the case of CCT specimen, several tests were conducted at displacement control mode with gauge length of 16 or 25 mm.

Table 1 Chemical composition of tested materials (wt.%)

	C	Si	Mn	P	S	Ni	Cr	Mo	Nb	V	Al	N	Cu	W
Mod.9Cr-1Mo	0.09	0.24	0.44	0.003	0.001	0.04	8.78	0.94	0.080	0.21	0.013	0.054	–	–
HCM12A	0.11	0.27	0.64	0.016	0.002	0.33	10.54	0.34	0.048	0.19	0.001	0.071	1.00	1.76

Table 2 Mechanical properties at room temperature

	0.2% yield stress	Tensile strength	Rupture elongation	Reduction of area
mod.9Cr-1Mo	528MPa	630MPa	26%	70%
HCM12A	617MPa	778MPa	23%	68%

Symmetrical triangular waveform was applied with a relatively short period (between 5s and 14s) in most of the tests but one test at 650℃ was conducted in unsymmetrical saw-type (slow-fast) waveform with a longer period consisted from tension-going time of 700 seconds and compression-going time of 7 seconds to examine the loading rate effect. Most tests employed fully-reversed loading with stain or stress ratio of -1 except one case employing the stress ratio of -0.74. Fatigue pre-cracking was introduced at room temperature in most tests.

In most tests, crack length was measured by direct current electrical potential method, although surface replication was also utilized in one series of tests. In the case of CCT specimens, displacement between two points 2 to 5 mm apart over the center of crack was measured and designated as crack opening displacement.

Load level was relatively high in all tests so that linear fracture mechanics can not be applied. Fatigue J-integral range, ΔJ_f in the field of nonlinear fracture mechanics was applied instead as a controlling parameter. ΔJ_f was experimentally evaluated from the load-crack opening displacement (load line displacement in the case of CT specimens) curves using the following formulae (Dowling and Begley, 1976, American Society for Testing Materials, 2001):

(for CCT specimen)

$$\Delta J_f = \frac{\Delta K_{eff}^2}{E} + \frac{S_p}{Bb}$$

$$S_p = \int_{\delta_0}^{\delta_{\max}} (P - P_0) d\delta - \frac{(P_{\max} - P_0)(\delta_{\max} - \delta_0)}{2}$$

(for CT specimen)

$$\Delta J_f = \frac{1+\alpha}{1+\alpha^2} \frac{2S_t}{Bb}$$

$$S_t = \int_{\delta_0}^{\delta_{\max}} (P - P_0) d\delta$$

$$\alpha = \sqrt{(2a/b)^2 + 2(2a/b) + 2} - (2a/b) + 1$$

where P and δ are load and crack opening displacement (load line displacement in CT specimens) , respectively. Ligament length (in each side in CCT) , crack length and thickness of the specimens are denoted by b, a and B, respectively. Subscripts 0 and $\max$ denote crack opening point and maximum load point, respectively. ΔK_{eff} is the effective stress intensity factor range corresponding to $P_{\max} - P_0$ and E is the Young's modulus of the material. Crack opening load was estimated from the load-displacement curve as a point where the slope changed discontinuously.

3.2 Test Result

In the case of load-controlled tests, crack growth was accelerated with the number of cycles. On the other hand, crack growth rate was fairly constant in the displacement-controlled tests because of decrease in load with crack growth. Correlation of crack growth rate with ΔJ_f is shown in Fig. 2. Except the slow-fast test data, crack growth rate at the same ΔJ_f is similar for both specimen types although small temperature dependency was observed. This indicates the fundamental effectiveness of ΔJ_f for estimating fatigue crack growth. Power-law relation holds for a whole range and a regression of all data except the slow-fast data led to the following equation:

$$da/dN = 3.00 \times 10^{-5} \Delta J_f^{\,1.47} \quad (da/dN \text{ in mm}, \Delta J_f \text{ in kN/m})$$

Most of the data points are within a band of factor of 2 from this line as shown in Fig. 2. In the slow-fast test excluded in the regression, crack growth rate was accelerated in the latter half of the test period and reached about 10 times as that in the fast-fast tests. This indicates the existence of the loading rate effect but more tests are required to quantitatively formulate it.

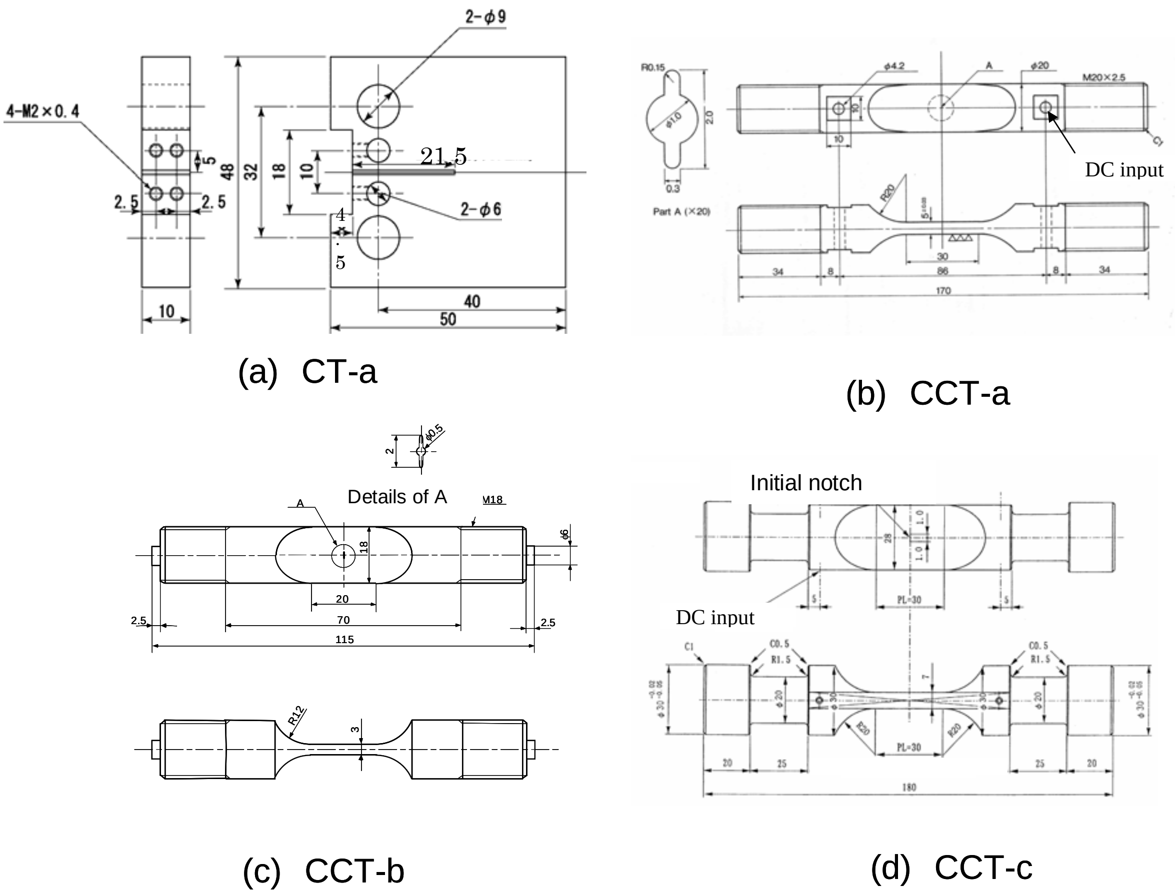

Figure 1 Geometry of test specimens used in fatigue crack growth tests

Table 3 Conditions of fatigue crack growth tests

Material	Specimen geometry	Control-mode	Temperature (℃)	Load ratio R	Period (s)	Number of cycles
Mod.9Cr-1Mo	CT-a (w=40,a=16.5,t=10)	Load	550	-1	5	6110
				-1		27000
			650	-1		1900
				-1		7345
	CCT-a (w=20, t=5)	Load	550	-1	10	15520
				-0.74	10	11280
			650	-1	10	540(no cg)
	CCT-b (w=18, t=3, GL=16)	Load	550	-1	10	2000
		Displacement		-1	10	500
			650	-∞	10	800
	CCT-c (w=28, t=7, GL=25)	Displacement	550	-1	14	750
			650	-1	14	915
				-1	707 (700t+7c)	538
HCM12A	CT-a	Load	600	-1	5	3155

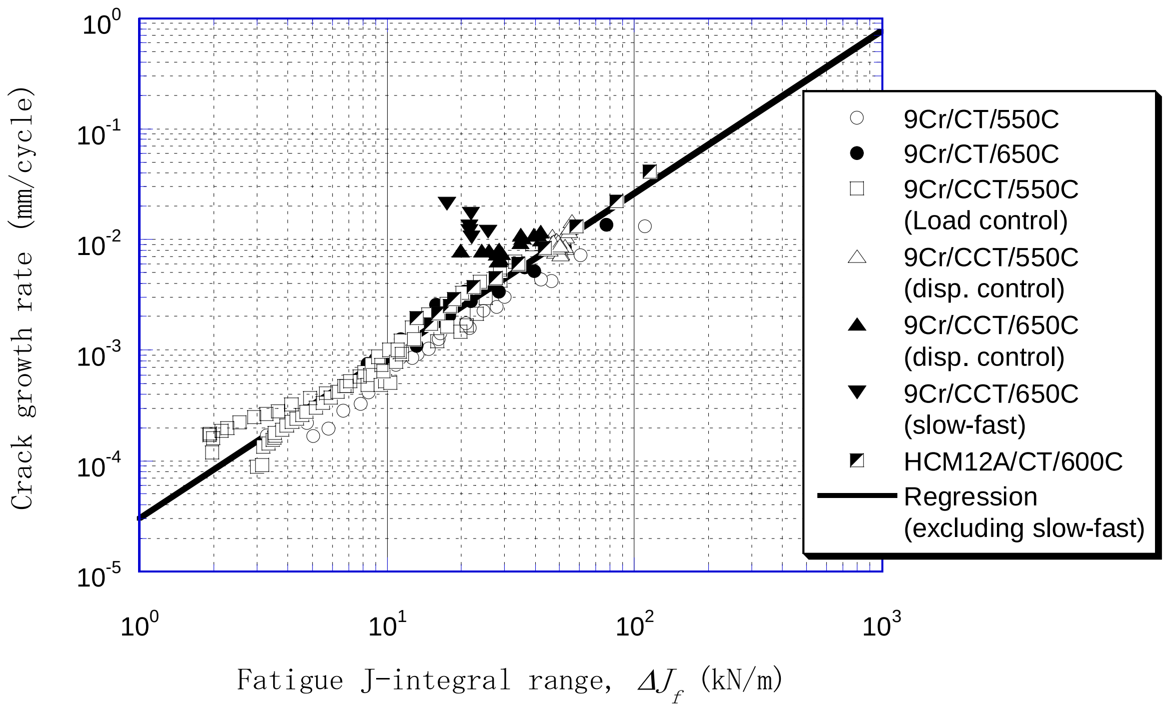

Figure 2 Plot of crack growth rate against fatigue J-integral range

4. CREEP CRACK GROWTH TESTS

4.1 Test Method

Totally 9 creep crack growth tests were conducted again using CCT and CT specimens both at 550 and 650℃ for modified 9Cr-1Mo steel and at 600℃ for HCM12A. Specimen geometry and test conditions are shown in Fig. 3 and Table 4, respectively. Instead of plane specimens used in fatigue crack growth tests, side-grooves were introduced in all specimens to raise the constraint. Even though, long time was spent before the initiation of crack growth particularly in the case of CCT specimens.

Creep J-integral, C^* was estimated from the crack opening displacement rate or load line displacement rate, $\dot{\delta}$ using the following formulae (Landes and Begley, 1976, American Society for Testing Materials, 2001):

$$C^* = \frac{n-1}{n+1}\frac{P\dot{\delta}}{2Bb}$$

$$C^* = \frac{n}{n+1}\frac{P\dot{\delta}}{Bb}\left(2 + 0.522\frac{b}{a+b}\right)$$

where *n* is the exponent of minimum creep rate equation. The minimum value at crack location was used as the thickness of the specimen.

4.2 Test Result

At the early stage of the tests, C^* was relatively large due to primary creep but cracks did not grow significantly. After taking a minimum value of C^*, crack growth rate started to grow with increase in crack length and C^*. Correlation between C^* and crack growth rate in this stage is shown in Fig. 4. In contrast to the fatigue crack growth, large dependence on specimen type and test temperature appeared in C^* –

crack growth rate relation. Crack growth rates in CT specimens were a order of magnitude higher than those in CCT specimens at the same value of C^*. This difference is considered to be generated as a result of difference in constraint as suggested by many works (O'Dowd and Shih, 1994, Budden and Ainsworth, 1999). As temperature rose, crack growth rate at the same C^* also increased drastically, probably due to decrease in ductility.

Comparisons of data from CT and CCT specimens at each material and temperature revealed that they are almost parallel and can be coincided with each other by shifting either CT or CCT data at some amount Result of such a trial is shown in Fig. 5, where data from CCT specimens were shifted upwards at an apparently optimum amount. It can be seen that unique relation could be obtained for each set of material and temperature. The amounts of shift were 12 and 5 for 550℃ and 650℃ data of modified 9Cr-1Mo steel and 10 for HCM12A data at 600℃. Analytical investigation (Budden and Ainsworth, 1999) predicted the increase in the constraint effect with the increase in the creep exponent and derived the ratio of crack growth rate in CCT specimens against more constrained CT-type specimens, as a function of creep exponent and normalized crack length. Crack growth rate ratio which could be obtained as an inverse of the above factors is plotted as a function of creep exponent obtained from standard creep equations (Japan Atomic Power Company, 1998, 2002) for both materials, with the predictions analytically obtained assuming the fracture process zone size of 0.01*a* (Budden and Ainsworth, 1999). In both analytical and experimental results, there is a clear and similar trend on

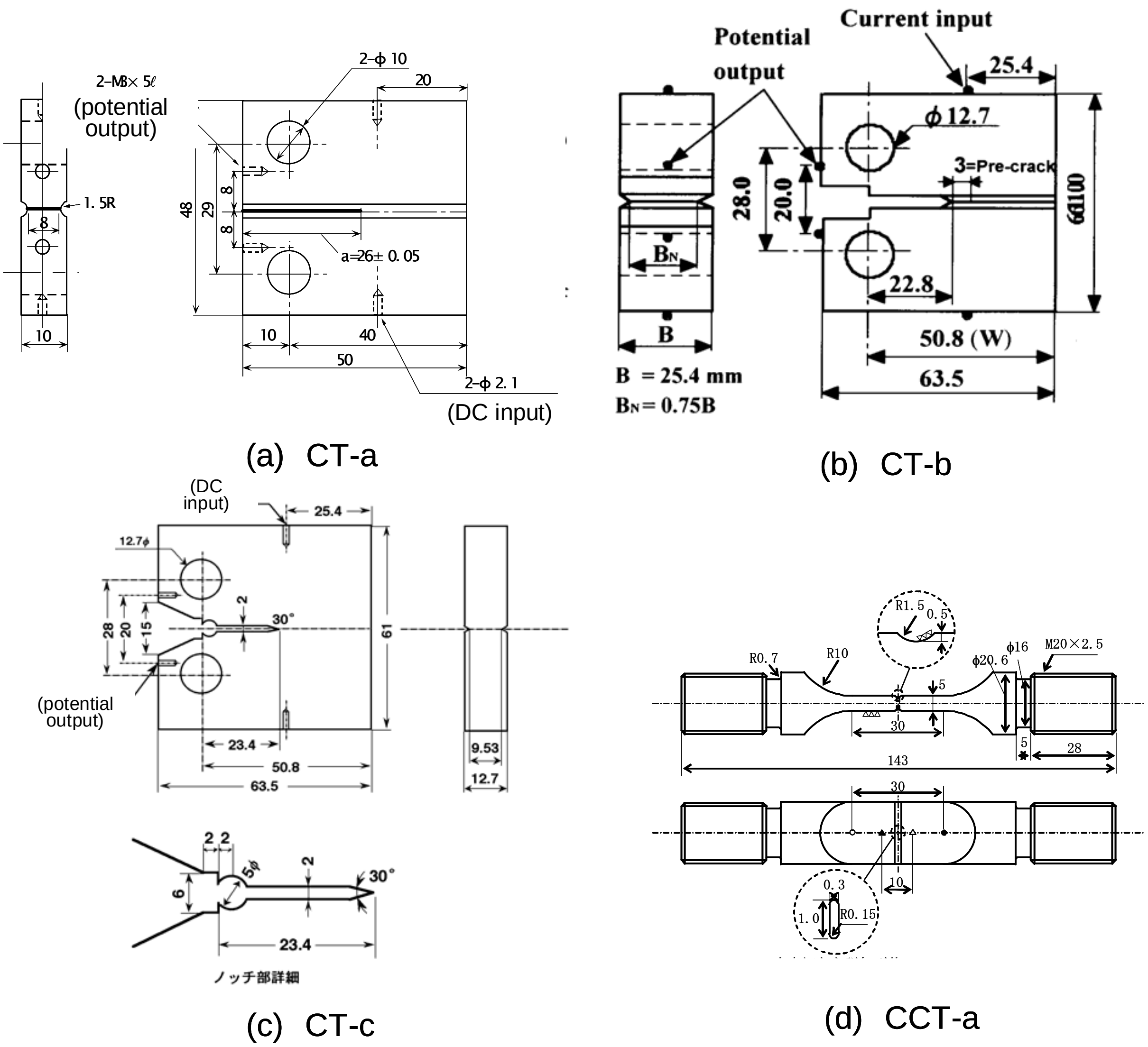

Figure 3 Geometry of test specimens used in creep crack growth tests

Table 4 Summary of creep crack growth tests

Material	Specimen type	Temperature (℃)	Test duration (h)
Mod.9Cr-1Mo	CT-a (w=40,a=16,t=10)	550	600
		650	337
	CT-b (w=51,a=23,t=25)	550	1006
		650	124
	CCT-a (w=20,t=5)	550	1020
			984
		650	552
HCM12A	CT-a (w=51,a=23,t=13)	600	2384
			2160
	CCT-a	600	697

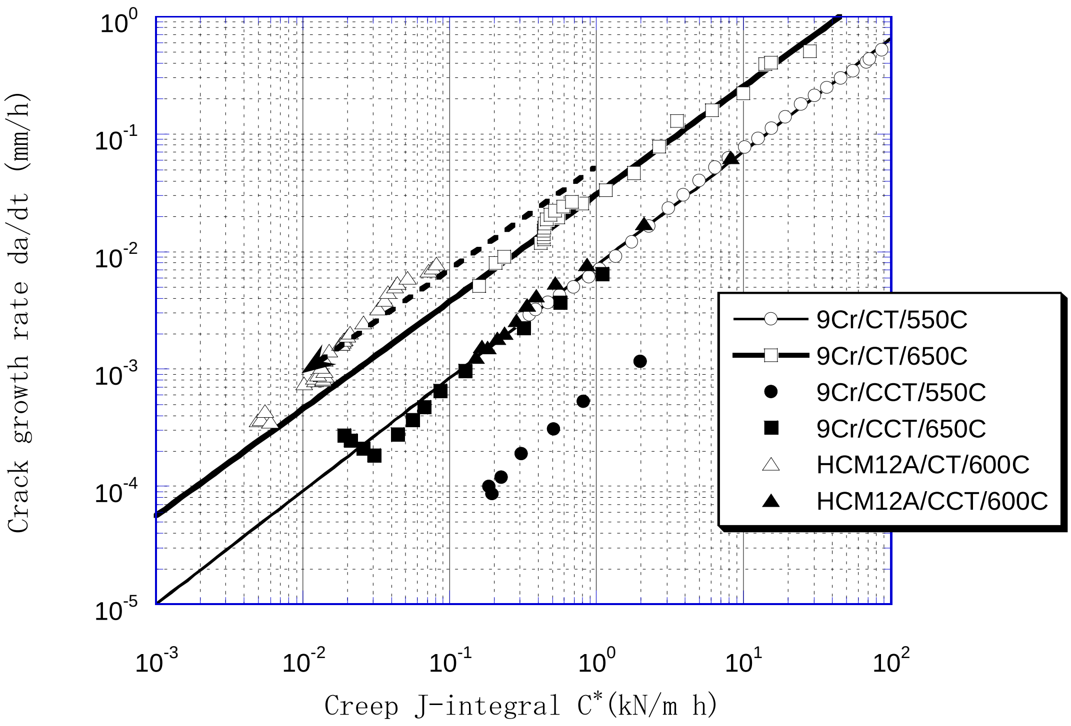

Figure 4 Relation between creep J-integral and creep crack growth rate

dependency of the crack growth rate ratio on the creep exponent. Examination of the correlation with uniaxial creep ductility would be useful to investigate the reason of material and temperature dependency.

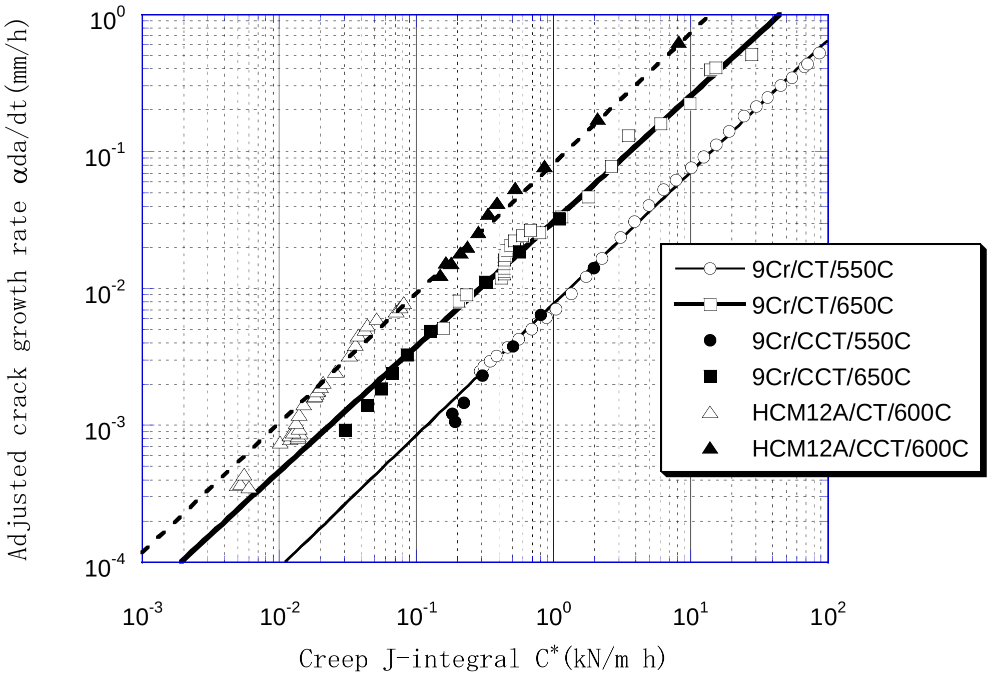

Figure 5 Relation between creep J-integral and adjusted creep crack growth rate

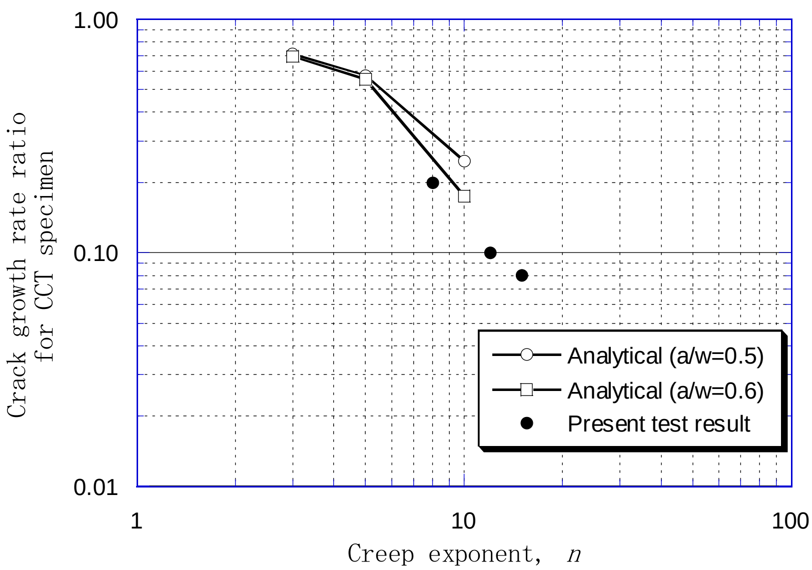

Figure 6 Relation between creep exponent and crack growth rate ratio for CCT specimen

5. CREEP-FATIGUE CRACK GROWTH TESTS

5.1 Test Method

Five creep-fatigue crack growth tests were conducted under trapezoidal waveform with hold time for 10 minutes or 1hour. Test specimens and conditions are summarized in Fig. 6 and Table 5, respectively. Both load-controlled and dsiplacement-controlled tests were included. Specimens are similar to those used in fatigue tests but side-groove was introduced in load-controlled tests. Only modified 9Cr-1Mo steel was tested mainly at 650℃.

In addition to fatigue J-integral range, creep J-integral range, ΔJ_c defined as a time integral of C^* was estimated from the variation of load and crack opening displacement or load line displacement during hold time using the following formulae:

$$\Delta J_c = \int_0^{t_H} \frac{n-1}{n+1} \frac{P\dot{\delta}}{2Bb} dt \qquad \text{for CCT specimen}$$

$$\Delta J_c = \int_0^{t_H} \frac{n}{n+1} \frac{P\dot{\delta}}{Bb} \left(2 + 0.522 \frac{b}{a+b} \right) dt \qquad \text{for CT specimen}$$

where t is time and t_H is hold time in each cycle. As in the case of creep crack growth tests, minimum thickness at cracked section was used for B.

5.2 Test Result

At first, crack growth behavior under creep-fatigue loading was compared with that under pure fatigue loading of the same loading condition except the hold time. In the case of load-controlled test using CT specimen, crack growth was significantly accelerated by introducing hold time even only for 10 minutes as shown in Fig. 6. Crack growth rate was accelerated by hold also in the case of displacement-controlled tests using CCT specimens but its degree was much smaller than the case of load-controlled test, as shown in Fig. 7. Some acceleration was also observed in the case of compressive hold test but its amount was also small. In the case of load-controlled tests with CCT specimen, crack grew in the direction nearly perpendicular to initial notch due to unknown reason.

In order to evaluate applicability of simple summation in terms of crack growth rate, crack growth rate was estimated by the following equation using experimentally estimated fatigue and creep J-integral ranges.

$$da/dN = C_f \Delta J_f^{m_f} + C_c \Delta J_c^{m_c}$$

where C_f and m_f are constants determined by fatigue crack growth tests whereas C_c and m_c are those by creep crack growth tests for the same material and temperature. It is assumed that m_c is close to 1.0 and integration of crack growth rate can be precisely approximated by the second term. Experimental crack growth rates are compared with predicted ones in Fig. 8 for both load- and displacement-controlled tests. Predicted rates agree with or were slightly smaller than the experimental ones in the case of displacement-control condition, whereas predictions were much faster than the measurements in load-controlled tests.

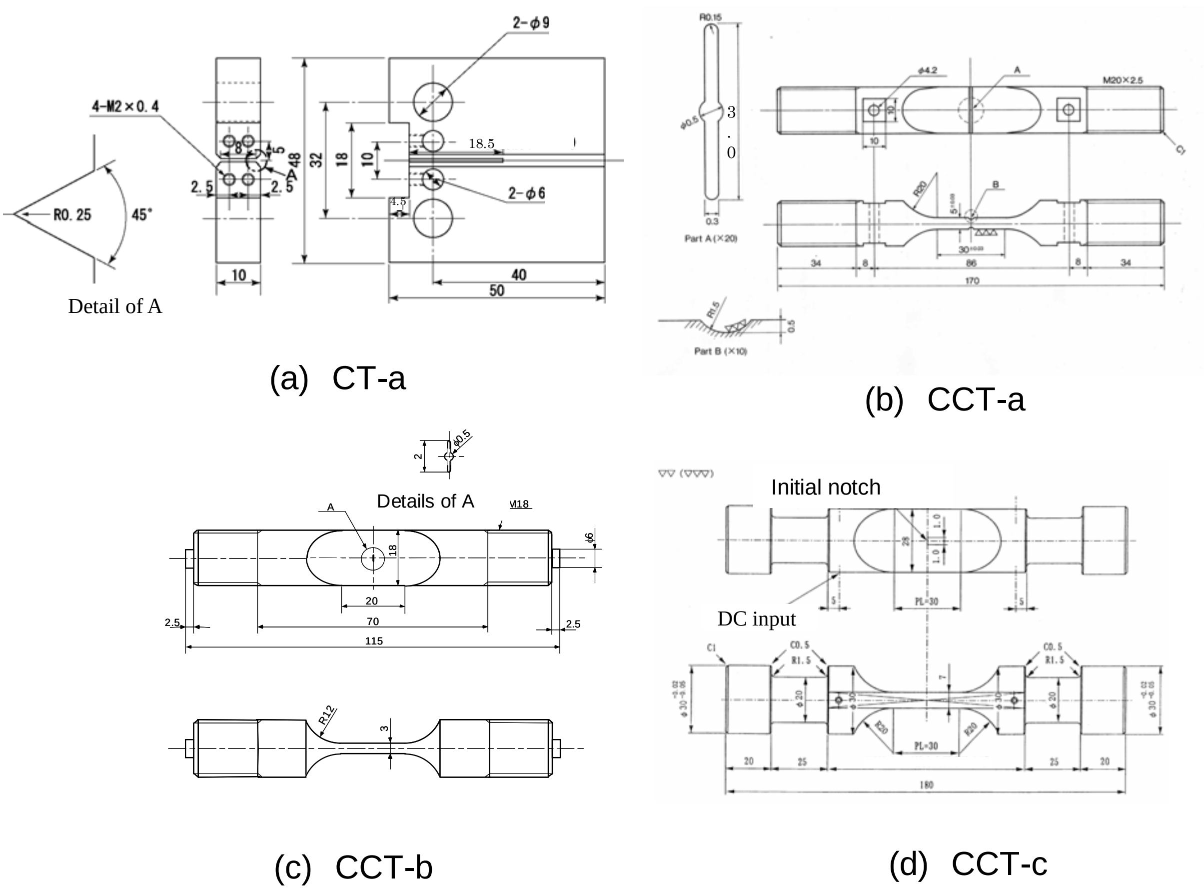

Figure 7 Geometry of test specimens used in creep-fatigue crack growth tests

Table 5 Summary of creep-fatigue crack growth tests

Material	Specimen type	Control -mode	Temper-ature (℃)	Hold position	Hold time (min)	Number of cycles
Mod.9Cr -1Mo	CT-a (w=40,a=13 ,t=10,SG)	Load	650	tensile	10	465
	CCT-a (w=20, t=5,SG	Load	550	tensile	10	7537 (no crack growth)
	CCT-b (w=18, t=4, GL=16)	Load	550	tensile	10	38
		Displac ement		compress ion	10	428
			650	compress ion	10	500
	CCT-c (w=28, t=7, GL=25)	Displac ement	550	tensile	10	660
			650	tensile	10	870
				tensile	60	523

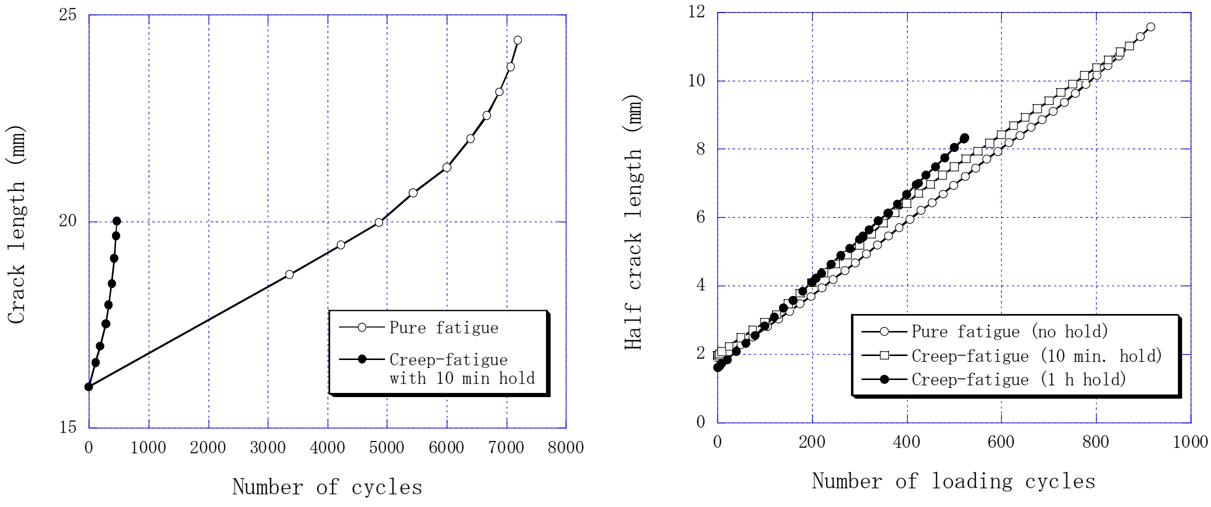

(a) CT specimen, load-control

(b) CCT specimen, displacement-control

Figure 8 Comparison of crack growth behavior in pure fatigue and creep-fatigue crack growth tests

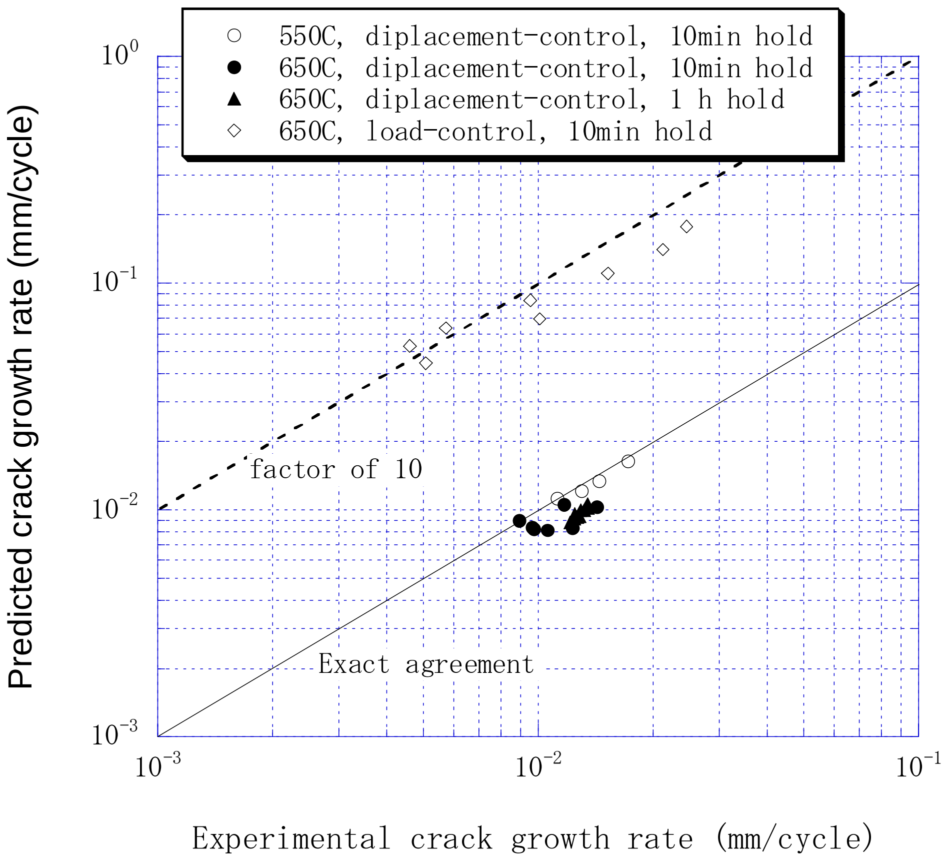

Figure 9 Comparison of experimental and predicted crack growth rates in creep-fatigue crack growth tests

6. CONCLUDING REMARKS

Crack growth tests under various loading conditions were carried out for two types of high-chromium ferritic steels widely used in power generation plants. It would be possible to summarize the results of the present study as follows;

(i) Fatigue crack growth rate was uniquely governed by fatigue J-integral range without a clear dependence on temperature and specimen type, although strain rate effect needs to be studied in more detail.

(ii) Creep crack growth rate was not fully determined by creep J-integral with large effects of specimen type and temperature. Specimen type-dependency observed in the present study was consistent quantitatively with the theoretical prediction.

(iii) Crack growth under load-controlled condition was largely accelerated by introduction of tensile hold but simple summation of fatigue and creep crack growth brought about considerable overprediction of crack growth rate.

Discussions given by other members of the WG are greatly appreciated.

REFERENCES

American Society for Testing Materials, (2000), E1457-00 Standard Test Method for Measurement of Creep Crack Growth Rates in Metals.

American Society for Testing Materials, (2001), E1820-01, Standard Test Method for Measurement of Fracture Toughness.

Budden, P. J. and Ainsworth, R. A., (1999), "The effect of constraint on creep fracture assessments," Int. J. Fracture, Vol. 97, pp. 237-247.

Dowling, N. E. and Begley, J. A., (1976), "Fatigue crack growth during gloss plasticity," ASTM STP 590, pp. 82-103.

Japan Atomic Power Company, (1998), High-temperature Structural Design Standard for Demonstration Fast Breeder Reactor (draft, in Japanese).

Japan Atomic Power Company, (2002), Report on the Study for Improvement of Design Method (in Japanese).

Landes, J. D. and Begley, J. A., (1976), "A fracture mechanics approach to creep crack growth," ASTM STP 601, pp. 1-20.

